TÉCNICO LISBOA

Thermoelectric generator from space to automotive sector- model and design for commercial and heavy duty vehicles

Sónia Cristina Azevedo Vale

Thesis to obtain the Master of Science Degree in

Aerospace Engineering

Supervisors: Prof. Pedro Jorge Martins Coelho
Prof. Carla Alexandra Monteiro da Silva
MSc. Lars Heber

Examination Committee

Chairperson:	Prof. Fernando José Parracho Lau
Supervisor:	Prof. Pedro Jorge Martins Coelho
Member of the Committee:	Prof. Tiago Alexandre Abranches Teixeira Lopes Farias

November 2015

Acknowledgments

I would like to start by thanking Lars Heber for giving me the opportunity to take part in the research at the Deutsches Zentrum für Luft und Raumfahrt, DLR and for his constant support throughout the learning process of this master thesis. Vielen Dank Lars.

I would like to thank professor Pedro Coelho, who despite the distance was always, without exception, available to help me with his immense knowledge. Obrigada professor Coelho.

I would like to thank professor Carla Silva and Ph. D. student João Ribau for the simulations they did for this master thesis. Additionally I would like to thank professor Carla for her friendly nature and kind of being. Obrigada.

Additionally, I would like to thank all the amazing people that I have met in Lissabon, Munich and Stuttgart during this past five years of studies in Aerospace Engineering. These people are irreplaceable and in some way or another turned these five years, in an unforgettable life experience. Not to forget my childhood friends, which always were there for me despite my constant absence from my home village. Thanks to each reencounter that felt like nothing changed.

To my family. Papá, Mamã e Sofia. Obrigada. Esta tese é dedicada a vocês.

Resumo

Apesar do aumento de combustíveis alternativos nos veículos ligeiros de passageiros, veículos comerciais e veículos pesados continuam a ser movidos a combustíveis fósseis. Os motores de combustão utilizados por estes veículos apenas convertem um terço da energia presente no combustível em potência de eixo. Os restantes dois terços são dissipados aproximadamente na mesma proporção para os gases de escape e líquido de refrigeração. Tendo em conta os elevados caudais mássicos característicos deste tipo de veículos, é ainda de esperar uma enorme quantidade de energia nos gases de escape. Este desperdício de energia identifica um problema que tem de ser investigado, a fim de melhorar a eficiência dos recursos e das emissões de CO_2. Esta tese propõe um gerador termoelétrico como uma solução promissora para a recuperação desta energia. Um gerador termoelétrico é baseado no efeito de Seebeck e converte energia térmica em energia elétrica. Um modelo numérico para um gerador termoelétrico foi desenvolvido e aplicado no sistema de gases de escape de um veículo comercial e um veículo pesado. Posteriormente foi realizado um estudo paramétrico à influência da geometria interna e externa do permutador de calor. Para esse efeito a potencia elétrica e potencia elétrica útil foram consideradas. Com base nestes dados a eficiência do sistema do gerador termoelétrico e a eficiência de recuperação do gerador termoelétrico são calculados e discutidos. Adicionalmente, a forma geométrica, em particular a altura da perna do termopar foi analisada. Os resultados obtidos nesta tese permitem tirar conclusões essenciais, relativamente ao desempenho global TEG.

Palavras-chave: Recuperção de calor, Gerador termoeléctrico, Efeito Seebeck, Veículos comerciais e pesados, Permutador de calor

Abstract

Despite the increase of alternative fuels for passenger cars, commercial and heavy duty vehicles continue to run on fossil fuel. The combustion engines used by these vehicles only convert around one third of the energy contained in the fuel into shaft power. The other two thirds are roughly dissipated equally into the exhaust gas and coolant. Given the high mass flow rates' characteristics for these vehicles a huge amount of energy is still expected to remain unused in the exhaust gas. This wasted energy presents a problem to be tackled in order to improve resource efficiency and CO_2 emissions. This master thesis proposes a thermoelectric generator (TEG) as a promising solution for this energy recovery. A TEG is based on the principle of the Seebeck effect and converts thermal energy into electrical power. A numerical model for a TEG was developed and applied to the exhaust gas system of both, a commercial and a heavy duty vehicle. Furthermore, a parametric study was performed on the influence of the heat exchanger's internal and external geometry. Herein the electrical and net output power were considered. Based on this data the TEG's system efficiency and TEG's recovery efficiency are calculated and discussed. Additionally, the geometric shape, particularly the thermocouple's leg height was analysed. The results obtained in this thesis allow the drawing of essential conclusions with regards to the overall TEG system performance which are essential to further studies.

Keywords: Waste heat recovery, Thermoelectric generator, Seebeck effect, Commercial and heavy duty vehicles, Heat exchanger

Contents

List of Tables

List of Figures

Nomenclature

Greek symbols

α	Seebeck coefficient, (VK^{-1}); Aspect ratio s/h
δ	Ratio t/l
η	Efficiency
γ	Ratio t/s
μ	Dynamic viscosity, ($kgs^{-1}m^{-1}$)
π	Peltier coefficient, (V)
ρ	Density, (kgm^{-3}); Electrical resistivity, (Ωm)
σ	Electrical conductivity, (Sm^{-1})
τ	Thomson coefficient, (VK^{-1})
φ	Correction factor for tubes of rectangular cross section
ξ	Darcy friction factor

Roman symbols

$\bar{a}_f$	Molar flow availability, ($Jmol^{-1}$)
$\bar{h_f}^0$	Enthalpy of formation per mole at Standard state, ($Jmol^{-1}$)
$\dot{m}$	Mass flow rate, ($\dot{m}$)
$\dot{n}$	Mol rate, ($mols^{-1}$)
$\dot{Q}$	Heat transfer rate, (W)
$\dot{V}$	Volume flow rate, (m^3s^{-1})
$\dot{W}$	Rate of work, (W)
A_c	Free flow area, (m^2)
c_p	Specific heat capacity, ($Jkg^{-1}K^{-1}$)

G	Mass velocity,($kgs^{-1}m^{-2}$)
j	Colburn factor
K	Thermal conductance, (WK^{-1})
k	Thermal conductivity, ($Wm^{-1}K^{-1}$)
m	Number of thermoelectric modules in x direction
n	Number of thermocouples in a thermoelectric module
Nu	Nusselt number
P	Output power, (W)
Pr	Prandtl number
Re	Reynolds number.
t	Fin thickness, (m)
V	Voltage, (V)
x, y, z	Rectangular coordinate system
Z	Figure of merit, (K^-1).
D_h	Hydraulic diameter, (m)
f	Fanning friction factor
L	Length, (m)
l	Fin length, (m)
p	Pressure, (Nm^{-2})
W	Width, (m)
A	Area, (m^2)
H	Height, (m)
h	Heat transfer coefficient, ($Wm^{-2}K^{-1}$); Fin height (m)
I	Current, (A)
i, j, k	Index counter
R	Resistance, (Ω)
s	Fin spacing, (m)
T	Temperature, (K)

Subscripts

A, B	Dissimilar materials
Al	Aluminium
b	Base
C	Carnot
c	Cold; Carnot
Cer	Ceramic
$conv$	Convection
Cu	Copper
CV	Control Volume
cw	Cooling water
ex	Exhaust gas
f	Fin; Fuel
h	Hot
int	Internal
L	Load
mp	Maximum Power
n	n-type material
oc	Open voltage
P	Products
p	p-type material
R	Reactants
ref	Reference condition
SS	Stainless steel
t	Thermal
TC	Thermocouple
TM	Thermoelectric module

Superscripts

ch Chemical contribution to availability

di Diffusion contribution to availability

th Thermomechanical contribution to availability

Overbar Average condition

List of Acronyms

CFD	Computational Fluid Dynamics.
GVW	Gross vehicle weight.
LHV	Lower heating value.
NASA	National Aeronautics and Space Administration.
RTG	Radioisotope Thermoelectric Generator.
RW	Reference mass.
TEG	Thermoelectric Generator.
UNECE	United Nations Economic Commission for Europe.
WHTC	World Harmonized Transient Cycle.
WLTC	Worldwide harmonized Light duty driving Test Cycle.
WLTP	Worldwide harmonized Light vehicles Test Procedure..
WVTC	World Harmonized Vehicle Cycle.

Chapter 1

Introduction

In recent years thermoelectric generators (TEG) working on the principle of the Seebeck effect emerged as a promising technology for waste heat recovery in the automotive industry. This technology allows to reuse waste heat and reduce energy consumption.

This chapter is organized as follows. It starts with a brief motivation of the investigated topic, in section 1.1 in which the technological potential is pointed out. Section 1.2 provides a review of the main work that has been developed by the scientific community with respect to this technology. Afterwards the objectives of this master thesis concerning the thermoelectric generator are presented in section 1.3. The chapter ends in section 1.4 with the thesis outline.

1.1 Motivation

In the automotive sector fossil fuels have assumed a position of undisputed leadership. Even with the non-oil alternatives predicted to increase from 5% in 2013 to 11% in 2035, the transport fuel demand will continue to be dominated by oil (89% in 2035)[1]. Subsequently, this high fossil fuel consumption contributes to the expected fuel scarcity in the nearly future and to the undesired global warming effect. As stated in [1] the total carbon dioxide (CO_2) emissions are expected to increase 25% between 2013 and 2035.

The non-oil alternatives mentioned before are specially intended for passenger cars. However, the commercial vehicles and heavy duty vehicles will still continue to be driven by oil in near future. From the fuel energy consumed by these vehicles, only one third is used to drive the vehicle. The remaining two thirds of the fuel energy are wasted as heat in the exhaust gas and in the coolant system. Reusing these energy losses would thus be a profitable way to improve fuel efficiency, since every wasted watt that is recovered to useful energy again is a gain. Consequently this would also result in lower CO_2 emissions. In conclusion it is imperative to analyse how the oil used by these vehicles can be utilized in a more efficient way.

For these reasons a major interest of research in the automotive sector is to develop a competitive and reliable key technology to recover this energy. In this context, a few years ago, the application of

a thermoelectric generator (TEG) in the exhaust gas system emerged as a possible solution. Although this technology is not new and the pioneer market for the TEG was the aerospace industry. On June 29th, 1961 NASA launched his first spacecraft that supported an RTG (Radioisotope Thermoelectric Generator), Transist-4A satellite, which was in operation for fifteen years [2]. Ever since then, RTGs have greatly enhanced and have allowed scientifically rewarding missions that could not have been performed otherwise.

The TEG works on the thermoelectric principle and converts thermal energy in electrical energy. When comparing to other environmentally friendly technologies the TEG presents distinctive advantages. Its biggest advantage is that it has neither moving parts nor refrigerators which makes the operation and maintenance of the whole system simple and less costly. TEGs also offer other major advantages, like the fact that they are extremely reliable, compact, light weighted and silent.

Owing these merits, the utilization of thermoelectric generators will remain a good prospect future automotive application. Therefore, further investigation is needed to achieve the goal of turning thermoelectric generators into “The waste heat recovery energy”.

1.2 State of the art

The Seebeck effect which is the underline scientific phenomena on which thermoelectric generator works was discovered in 1821 by Thomson J. Seebeck. This effect stated that a circuit made from two dissimilar materials with their junctions at different temperatures produce a potential difference. Thirteen years later, in 1834 the Peltier effect was discovered by Jean Peltier and later in 1854, the Thomson effect was discovered by William Thomson. After these findings, the interest in thermoelectric quickly started to expand.

The earliest studies on thermoelectric generation as a waste heat recovery technology in automotive emerged in 1963. However, only in Germany in 1988 Birkholz et al. [3] built the first thermoelectric generator for automotive by using 90 couples of $FeSi_2$. The p-type and n-type $FeSi_2$ thermocouples were columnar with a cross section area of 1 cm^2 and a length of 1.3 cm. Their TEG was tested on a Porsche 944 under full engine power and a output power of 58 watts was obtained.

At the same time, in the USA, Bass et al. [4], one of the Hi-Z Company’s founder, also started studies in order to develop a TEG for the exhaust gas in a diesel truck. In 1993 they presented their TEG prototype made with 72 Hi-Z 13 modules. Each of these modules had a constant cross sectional area of 5.3 cm^2 and 0.5 cm height. This TEG was tested on a 14 L Cummins NTC 350 and a maximum output power of 1068 W was obtained when driving at 223.7 kW and 1700 min^{-1}.

In Japan the interest to apply thermoelectric to exhaust gas of vehicles also awoke. In the late 90s Ikoma et al. [5], at the Nissan research centre, presented a prototype generator for gasoline engine vehicles using SiGe elements. The generator was made with 72 SiGe modules. The modules used had a cross section area of 0.20 cm^2 and a length of 0.92 cm. The TEG was tested on a combustor bench where the exhaust gas got introduced into the generator corresponded to a 60 km h^{-1} hill climb mode of a 3000 cm^2 gasoline engine vehicle. The output power measured under this condition was 35.6 W.

These early studies proved that the TEG has potential to be applied in the vehicle exhaust gas system and a massively growing interest in these devices arises in the automotive industry. Besides, the increasingly growing demand for such technology spurred a growing interest in scientific community where several studies have been carried out. This research area can be divided in two main parts: experimental studies and theoretical analyses and numerical methods. Both are presented next.

Experimental studies

Experimental analyses have the advantage of examining the real performance of a TEG system on vehicles. Some of them are listed below. Thacher et al. [6] conducted experiments on a prototype automotive exhaust TEG system installed in a GMC Sierra pick-up truck and found out that the thermal management, most particularly the coolant fluid temperature, plays a very important role in the thermoelectric generator system. Hsu et al. [7, 8] tested the performance of TEG system which was connected to the middle section of an exhaust pipe of a Chrysler Neaon 2000 cm^3. The TEG was made by eight Bi_2Te_3 TE modules. When subjected to the engine rate of 3500 min^{-1}, the system generated a measured maximum power of 44.13 W. Recently Liu et al. [9] designed and constructed a new system called "four-TEGs". This system was assembled into the prototype vehicle called "Warrior". Through the road test and revolving drum test table, characteristics of the system such as hot-side temperature, cold-side temperature, open circuit voltage and power output were studied. In and Lee [10] conducted two tests on a common diesel engine with a cubic capacity of 2.2 L where the performance of a thermoelectric module was measured using a rig test device and an engine dynamometer. The experimental results confirmed that the temperature difference between the two ends of the TEG and the flow rate of the exhaust gas are major factors for determining the power generation performance of a thermoelectric module.

Theoretical analyses and numerical methods

Theoretical analysis and numerical modelling are also essential tools for the progress and development of TEG applications, providing a deeper insight in the physical processes underlying transport phenomena. Up to this point the numerical models have been mostly developed on a component level without the deeper comprehensive of the system and its iterations.

The heat exchanger represents one of this components, that attracts specially interest due to its imperative improvements. The energy transfer from the exhaust gas to the thermocouples represents a big barrier in the overall performance of the TEG. In order to find a solution for this problem, several studies were conducted on this topic.

Lu et al. [11] investigated two types of heat transfer enhancements for an exhaust gas heat exchanger, rectangular offset strip fins and metal foams. They used the net power output as main comparative parameter. Bai et al. [12] and Lu et al. [13] also investigated this topic, with the purpose of finding a heat exchanger internal structure that best meets the overall requirements for their applications on a TEG. Su et al. [14, 15] used computational fluid dynamics simulations to investigate the thermal performance of heat exchangers with different internal structures and thickness, with the aim of obtaining higher interface temperatures and thermal uniformity. Likewise Zhou et al. [16] investigated the influence of a new heat exchanger design with a cylindrical shell and straight fins. In all these mentioned studies

the thermoelectric modules as well as their respective connection parts where not used as a simulated parameter. For the purpose of obtaining the output power of the TEG with respect to the heat exchanger performance, they used existing commercial modules.

Apart from the heat exchanger the simulation and prediction of the thermoelectric modules' behaviour under different boundary conditions is essential for the development of the TEG. For this purpose Niu et al. [17], developed two 3D numerical models to study the thermocouple behaviour under different modelling boundary conditions. They conclude that these can strongly influence the modelling results. They also investigated in detail the influence of the thermocouple's shape on its performance and concluded that the temperature gradient could be enhanced if a proper cross section area is used. Abdelkefi et al. [18] developed and validated an analytical electro thermal model for thermoelectric modules. For different hot side temperatures and for different clamping forces the electrical output power from a single thermocouple was measured and analysed. Chen et al. [19] did a study on the same topic and analysed essentially the influence of the material properties on a single thermocouple.

Only a few studies concerning the overall system modelling were performed. This may arise from the fact that in this preliminary stage its quite difficult to make a feasible estimation of the overall components of the TEG in order to assess and study the overall TEG system performance. However these system studies are crucial. Some of the few studies on this matter are listed next. Yu et al. [20] developed a numerical model for TEG and analysed its behaviour for constant and dynamic driving conditions. To simulate the thermoelectric modules they used 16 commercial Bi_2Te_3 HZ-20 [21] thermoelectric modules. It was found that the vehicle speed is a significant factor affecting the TEG performance for waste heat recovery. Gou et al. [22] in their study developed a theoretical dynamic model for a thermoelectric generator with a finned heat exchanger. The dynamic response on the maximum output power and efficiency of the TEG was analysed by means of step changes of the heat reservoir temperature and mass flow rate. Tatarinov et al. [23] did a similar work but instead of using step changes for the hot side temperature and mass flow rate he applied his model on four different car driving patters, two from Europe and two form the USA. Kumar et al. [24, 25] in their studies also developed a numerical model for thermoelectric generator but for steady state analysis. For the baseline analysis they took the average inlet conditions from a typical light duty vehicle. Wang et al. [26] also presented a steady state mathematical model of a thermoelectric generator by using the exhaust gas of vehicles as heat source. Their model was applied to several points taken from the FTP-75 (federal test procedure for the city driving cycle).

Even though that application of thermoelectric generators as a waste heat recovery system is only at the stage of theoretical research and experimental demonstration, it seems to offer great potential for future developments. In order to meet the ambitious goals set for the automotive industry, further investigation needs to be continued to put this new waste heat recovery technology on a industrial and commercial scale.

1.3 Objectives

From the literature reviewed in the previous section, it can be recognized that most studies have mainly focused on the analysis of the heat exchanger or the thermocouples separately. As it was seen above, there are only a few works that simulated the complete TEG system model.

Subsequently, to fill this gap, the objective of this master thesis is to develop a numerical model of a thermoelectric generator for the application in the exhaust gas of commercial and heavy duty vehicles.

The developed numerical method should be furthermore used to perform a parametric study on the heat exchanger. This parametric study should result in a first prediction of the output power which can be expected from these thermoelectric generators when applied in the exhaust gas system of the vehicles mentioned before. A first estimation of the TEG's system efficiency and the TEG's recovery efficiency should also be presented. Additionally, the thermocouple's influence on the TEG should be investigated.

1.4 Thesis Outline

This master thesis is organized as follows:

Chapter 2 presents a brief review and some main insights on the thermoelectric device to understand the physics behind this work. Subsequently, the numerical model developed to simulate the thermoelectric generator in the exhaust gas system of commercial and heavy duty vehicles is presented and explained. To complete this chapter the numerical model is validated against experimental data.

Chapter 3 introduces a few automotive concepts which concern the TEG application. The vehicles' classification by weight and the driving cycles used by the European law are presented. A brief analysis of the diesel exhaust gas system also is given. Finally, the target study is selected and the overall vehicle performance is simulated in order to get the necessary data which will be used as input in the next chapter.

Chapter 4 starts with an energetic and availability analysis in order to evaluate the energetic potential existent in the exhaust gas of the selected vehicles presented before. Next the numerical model developed in chapter 2 is applied. With this numerical model a parametric study is carried out to evaluate the impact of the heat exchanger on the overall performance of the thermoelectric generator. Within this study the first reference values for the electrical output power expected from a TEG as well as the TEG's efficiency are obtained. The chapter end's with an analysis of the thermocouple's influence on the TEG.

The thesis ends in chapter 5 with an overview of the main achievements of this master thesis and some suggestions of future work that can be developed in this area of expertise.

Chapter 2

Model development: Thermoelectric Generator

A TEG which converts thermal energy into electrical energy, can be divided into three main parts, the thermocouples, the hot side and the cold side. In this master thesis a TEG for an automotive exhaust gas system will be developed, by using the vehicles exhaust gas as the heat source and the coolant as the cold sink. A numerical simulation is used to predict the performance of the TEG system.

This chapter is organized as follows. Section 2.1 starts with some background definitions concerning the thermoelectric effect, which is of fundamental importance to understand the fundamentals of the thermoelectric system. Section 2.2 refers to the performance and efficiency of thermoelectric. The section that follows, section 2.3 provides a detailed description of the thermoelectric thermal and electrical behaviour. Finally in section 2.4, the description and validation of the numerical model of the thermoelectric generator are presented.

2.1 Physical phenomena of thermoelectrics

The thermoelectric effect is the underlying scientific phenomenon that underpins this master thesis. This term encompasses three separate but interrelated thermoelectric phenomena: the Seebeck effect, the Peltier effect and the Thomson effect. The interrelationships between these three effects are given by the Thomson (or Kelvin) relations that will be presented further ahead.

Seebeck effect

The Seebeck effect states that whenever two dissimilar thermoelectric materials are joined into a loop, with the two junctions maintained at different temperatures, a temperature induced electrical potential also known as electromotive force (emf) is generated. The generated electromotive force represents the Seebeck voltage V_{oc} and is defined as

$$V_{oc} = \alpha_{AB} \Delta T \tag{2.1}$$

where α_{AB} (V K^{-1}) represents the relative Seebeck coefficient of two dissimilar conductors A and B and ΔT (K) represents the temperature difference between the junctions as stated in equation 2.1. The voltage in the open circuit is proportional to the temperature difference and depends on the type of conduction material, though it is not a function of the temperature distribution along the conductor.

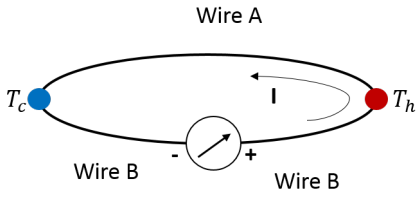

Figure 2.1: Schematic of the Seebeck effect represented on a thermocouple.

The Seebeck effect shown in figure 2.1 is a basic principle of thermoelectric and of considerable practical importance for creating an efficient thermoelectric generator. Consequently, within the framework of this master thesis, more detailed description of this effect seems proper and is presented hereafter.

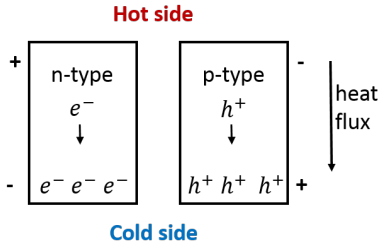

Figure 2.2: Schematic of the n-type and p-type thermoelectric material behaviour.

Semiconductors are often used as thermoelectric materials. Thermoelectric materials are materials that show the required properties which enable them to be used to convert thermal energy into electricity and vice versa. Often, impurities are added to semiconductors, a phenomenon known as “doping”, with the aim of increasing the number of charge carries within it. There are two main types of doping, the negative type (n-type) and the positive-type (p-type). In the first type of doping valence electrons are added and in the second type, valence electrons are removed. When a semiconductor is subjected to two different temperatures at their ends, together with the heat flow through the pellets, the charge carriers flow in the same direction, from the warmer side to the colder one as seen in figure 2.2. In the n-semiconductor the electrons will tend to migrate towards the cold side, and in the p-semiconductor leg the holes will move toward the cold side. This creates a voltage gradient between the legs. It is worth noting that the Seebeck effect is a contact phenomenon that only occurs through connection of two dissimilar thermoelectric materials.

Peltier effect

The Peltier effect states that if an electrical current flows across a junction between two dissimilar materials, heat must be continuously added or subtracted at the junction in order to keep its temperature constant. The rate of heat absorbed or rejected at a junction due to the Peltier effect is proportional to

the electrical current flow and is given by

$$\dot{Q}_{Peltier} = \pi_{AB} I \tag{2.2}$$

where π_{AB} (V) represents the relative Peltier coefficient of two dissimilar materials, a property that determines the magnitude of the heating or cooling that occurs at a junction of the two dissimilar materials. I (A) represents the electrical current that flows through the thermocouple. Similarly to the Seebeck effect, the Peltier effect is also a contact phenomenon that occurs across the contact boundary between two dissimilar materials. It is worth mentioning that the Peltier heating or cooling is reversible between heat and electricity. This means that heating (or cooling) will produce electricity and electricity will produce heating (or cooling) without energy dissipation.

Thomson effect

The Thomson effect states that whenever a current flows in a wire with a temperature gradient, heat is absorbed or liberated across the wire depending on the material and the direction of the current. The rate of heat absorbed or released along the length of the wire due to the Thomson effect is given by

$$\dot{Q}_{Thomson} = \tau I \Delta T \tag{2.3}$$

where τ (V K^{-1}) denotes the Thomson coefficient, I (A) is the current and Δ T (K) is the temperature difference between the two ends of the wire. The Thomson heat is reversible and should not be confused with the Joule heating, an irreversible effect in which the passage of an electrical current through a conductor releases heat.

Thomson (or Kelvin) relationships

To fulfil this thermoelectric effect description, the interrelations between the three thermoelectric effects are presented.

The Peltier coefficient is related to the Seebeck coefficient by the following equation

$$\pi_{AB} = \alpha_{AB} T \tag{2.4}$$

The Thomson coefficient is related to the Seebeck effect by

$$\tau_A - \tau_B = T \frac{d\alpha_{AB}}{dT} \tag{2.5}$$

In equations 2.4 and 2.5, A and B represent the two dissimilar conductors. Both equations are known as the Thomson (or Kelvin) relationships.

2.2 Figure of merit and efficiency

The figure of merit (Z) represents the inherent relationship between the main material properties (both electrical and thermal) that must be considered when assessing the performance of a given thermoelectric material. It is defined as

$$Z = \frac{\alpha^2}{\rho k} \tag{2.6}$$

where α represents the Seebeck coefficient, k is the thermal conductivity and ρ the electrical resistivity.

The figure of merit has units of reciprocal temperature (K^{-1}), however it is often multiplied by the absolute nominal temperature in order to obtain a dimensionless parameter, known as ZT. Representing the thermoelectric material performance in dimensionless units has the advantage of allowing a direct comparison of the potential efficiency of thermoelectric devices with different materials, even for different operating temperature range.

As seen in equation 2.6, since Z is proportional to the square of the Seebeck coefficient, increasing the Seebeck coefficient impacts overall material performance the most. For that reason, it is desired that α, which represents the voltage potential that can be produced given an applied temperature gradient, should be as high as possible.

On the other hand, k and ρ are inversely proportional to Z, and for that fact, low values of thermal conductivity and electrical resistivity represent higher values of Z. A low thermal conductivity helps to retain heat at the junctions of the material and maintain a large temperature difference, while low electrical resistivity diminishes the amount of heat loss by the Joule heating, two desirable behaviours in a thermoelectric material.

All of the material properties described so far are strongly temperature-dependent. So it is of best interest to choose the materials with the highest figure of merit in the range of temperature of interest.

The thermal efficiency of a TEG is the amount of electrical power generated for a given amount of heat input. It is given as

$$\eta_t = \frac{P_{electrical}}{\dot{Q}_h} \tag{2.7}$$

The first law of thermodynamics states that energy is neither created nor destroyed, so that the thermal efficiency of a power cycle is always less than or equal to 1. The maximum theoretical value of η_t is given by the Carnot efficiency:

$$\eta_C = 1 - \frac{T_c}{T_h} \tag{2.8}$$

where T_h and T_c represent the hot and cold junction temperatures, respectively.

Taking this into consideration, it is useful to represent the thermal efficiency of a TEG as a function of the Carnot efficiency as follows [27]

$$\eta_t = \eta_C \frac{\frac{R_L}{R_{int}}}{\left(1 + \frac{R_L}{R_{int}}\right) - \frac{\eta_c}{2} + \frac{\left(1+\frac{R_L}{R_{int}}\right)^2}{ZT_h}} \tag{2.9}$$

where R_L is the load resistance and R_{int} is the thermocouple's internal resistance. The efficiency given

by equation 2.9 can be maximized for a maximum conversion efficiency or maximum power efficiency. The maximum power efficiency, which is of interest for this work, is achieved when R_L equals R_{int} as will be demonstrated in 2.3.2. Introducing this relation in equation 2.9 the maximum power efficiency is obtained

$$\eta_{mp} = \eta_C \frac{1}{2 - \frac{\eta_C}{2} + \frac{4}{ZT_h}} \tag{2.10}$$

Figure 2.3 represents the maximum power efficiency as a function of T_h for three different Z values with T_c fixed at 95^oC. The actual material's Z values available for industrial application are nearly Z=0.001, although an effort to achieve higher Z values is underway.

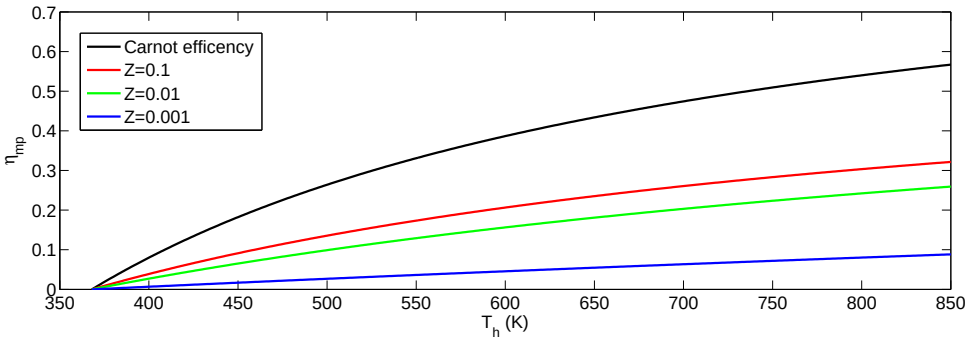

Figure 2.3: Maximum power efficiency as a function of T_h, for different Z values, with T_c=95 ºC.

2.3 Thermocouple

A thermocouple is the main building block of a thermoelectric power generator. A thermocouple is composed of a pair of p-type and n-type semiconductor legs which are connected at least at one point, figure 2.4 (a). Multiple legs of p-doped and n-doped semiconductors are connected electrically in series and thermally in parallel to form a thermoelectric module, figure 2.4 (b). To connect the multiple legs, electrical conducted strips are used. These strips allow the current to flow through the legs. In addition, to ensure electrical insulation and structural support of the thermoelectric module, ceramic strips are used, as represented in figure 2.4 (c).

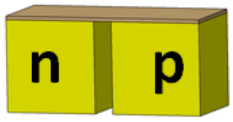

(a) Thermocouple design.

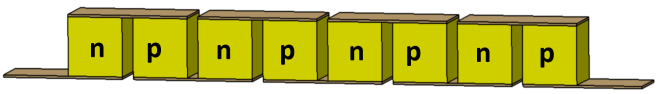

(b) Thermoelectric module design.

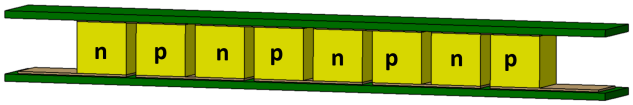

(c) Thermoelectric module design and ceramic plates.

Figure 2.4: Thermoelectric components design.

The operational principle of a single thermocouple can be slit in two, the thermal behaviour and the electrical behaviour. Subsequently these two are couple with each other as seen in figure 2.5. Next, a detailed description of the thermal and electrical behaviour of a single thermocouple is presented.

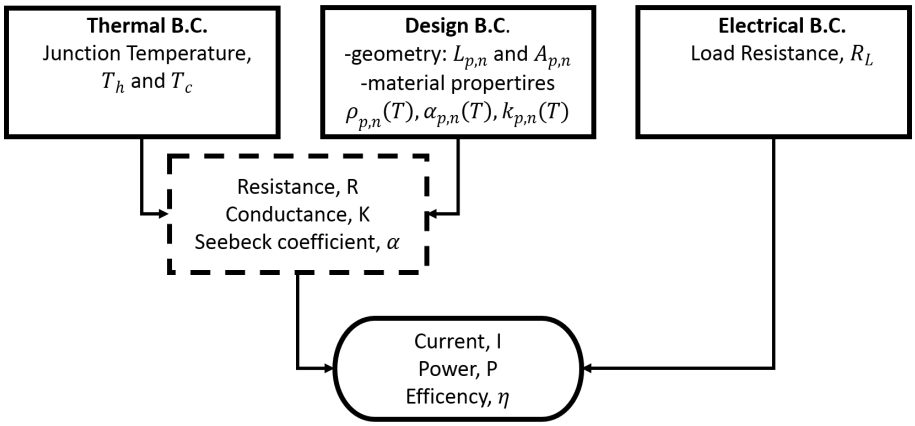

Figure 2.5: Schematic of the relation between the thermocouple's electrical and thermal behaviour.

2.3.1 Thermal behaviour

To properly perform a thermal analysis the practical aspects of the underlying complex phenomenon must be known and so assumptions and simplifications must be made. Taking that into consideration, steady state is assumed, the heat losses due to radiation are neglected, the gap between the thermocouples is assumed perfectly isolated, the axial heat conduction within the thermocouples is ignored since the heat transfer in the y-direction is assumed to dominate and the current flow in the thermocouple is also assumed to be one-dimensional in the y-direction.

Following these assumptions, the energy balance equation for an infinitesimal element dy, depicted in figure 2.6, can be given by

$$\dot{Q}_y - \big(\dot{Q}_y + \frac{d\dot{Q}_y}{dy}dy\big) + \frac{I^2\rho}{A}dy = 0. \tag{2.11}$$

The first term in equation 2.11 represents the heat transfer across the surface of the element. The second term in 2.11 represents the Joule heating effect, associated with the release of heat due to the passage of the electric current through the leg. The Joule heat is distributed throughout the element therefore half the heat flows towards one side and the other half goes towards the opposite side of the thermocouple. The boundary conditions are $T(y)|_{y=0} = T_h$ and $T(y)|_{y=L} = T_c$ and once applied to equation 2.11 yield

$$T(y) = -\frac{I^2\rho y^2}{2A^2k} + \big(\frac{T_c - T_h}{L} + \frac{I^2\rho L}{2A^2k}\big)y + T_h \tag{2.12}$$

which represents the temperature distribution across the thermocouple.

The energy balances at the hot and cold junctions of the thermocouples are given, respectively by

$$\dot{Q}_h = (\alpha_p - \alpha_n)T_h I + \big(-k_p A_p \frac{dT}{dy}|_{y=0} - k_n A_n \frac{dT}{dy}|_{y=0}\big) = 0 \tag{2.13}$$

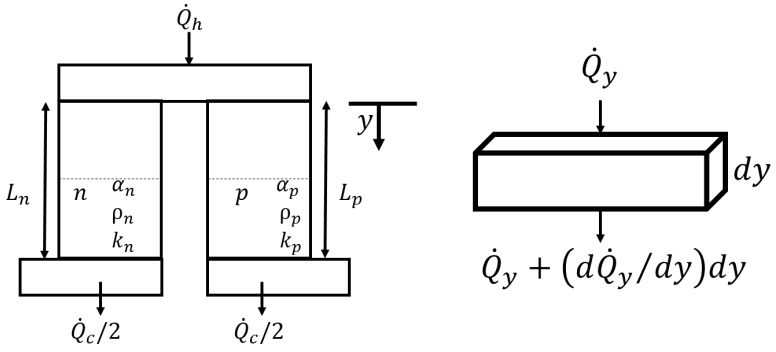

Figure 2.6: Schematic of the heat rate in a thermocouple.

$$\dot{Q}_c = (\alpha_p - \alpha_n)T_c I + \big(- k_p A_p \frac{dT}{dy}|_{y=L} - k_n A_n \frac{dT}{dy}|_{y=L}\big) = 0 \tag{2.14}$$

In equations 2.13 and 2.14 the first term accounts for the Peltier heat, which using the relation given by 2.4, can be written in function of the Seebeck coefficient. The second term represents the Fourier's law of thermal conduction at the boundaries, $y = 0$ and $y = L$, respectively. From equation 2.12, the Fourier's thermal conduction terms in 2.13 and 2.14 can be determined. Subsequently the total heat flow rates through the hot and cold junctions of the thermocouples are given as

$$\dot{Q}_h = \alpha T_h I - \frac{1}{2} I^2 R_{int} + K(T_h - T_c) \tag{2.15}$$

$$\dot{Q}_c = \alpha T_c I + \frac{1}{2} I^2 R_{int} + K(T_h - T_c) \tag{2.16}$$

where R_{int} represents the internal (electrical) resistance and K the thermal conductance from the thermocouples, and are given as follows

$$R_{int} = \frac{\rho_p L_p}{A_p} + \frac{\rho_n L_n}{A_n} \tag{2.17}$$

$$K = \frac{k_p A_p}{L_p} + \frac{k_n A_n}{L_n} \tag{2.18}$$

In 2.15 and 2.16, α_{pn} represents the difference in Seebeck coefficient of the two thermocouple's legs, T_h and T_c are the temperatures at the hot and cold junctions respectively and I is the electric current in the circuit.

2.3.2 Electrical behaviour

Due to the Seebeck effect, the temperature drop across the thermocouple's legs induce a voltage drop. Moreover, it is known that doped semiconductors have an associated internal resistance. Consequently the thermocouple can be treated as a temperature controlled voltage source in series with an internal resistance, as depicted in figure 2.7.

Adding a load resistance (R_L) to the circuit, the electrical power generated by the thermoelectric

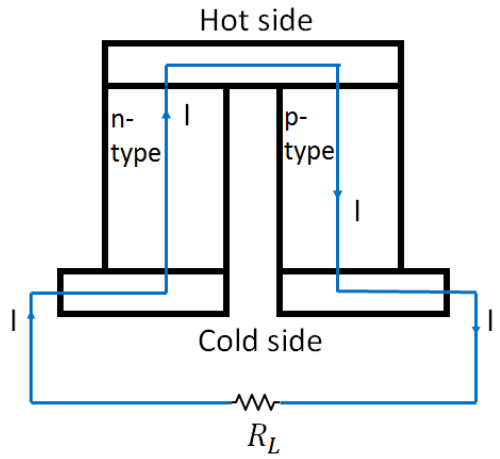

(a) Schematic of the thermocouple in power generation mode.

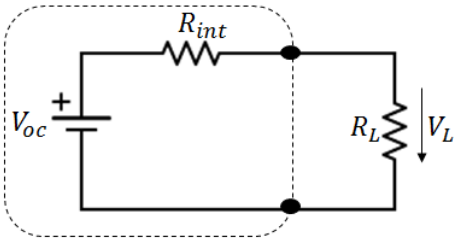

(b) Schemactic of the electrical circuit model of a thermoelectric generator.

Figure 2.7: Schematic of the thermocouple's electrical behaviour.

couple is given by the product of the voltage across the load resistance and the current in the circuit, as

$$P = V_L I = \frac{V_{oc}^2 R_L}{(R_L + R_{int})^2} \tag{2.19}$$

In order to obtain the maximum power output the derivative of 2.19 with respect to the resistance ratio R_L/R_{int} is set to zero, and the relationship for maximum power is obtained

$$R_{int} = R_L \tag{2.20}$$

Under the stated conditions, the load current for maximum power generation (I_{mp}) can be determined by

$$I_{mp} = \frac{\alpha_{pn}\Delta T}{2R_{int}} \tag{2.21}$$

and the load voltage equals half the open circuit voltage, as formulated in

$$V_{L,mp} = \frac{V_{oc}}{2} = \frac{\alpha_{pn}\Delta T}{2} \tag{2.22}$$

Finally, combining equations 2.19 and 2.20 the maximum output power can be obtained

$$P_{mp} = \frac{(\alpha_{pn})^2 \Delta T^2}{4R_{int}} \tag{2.23}$$

2.4 Thermoelectric system modelling and validation

Not available.

2.4.1 Thermoelectric generator design

Not available.

2.4.2 Energy equations

Not available.

2.4.3 Hot side and cold side

Not available.

2.4.4 Thermoelectric modelling

Not available.

2.4.5 Thermal resistance network

Not available.

2.4.6 Numerical approach and validation

Not available.

Chapter 3

Case study

Within the automotive industry there are several ways to categorize vehicles. In this chapter the vehicles' weight class will be considered. This vehicle classification is the one used to define the permissible level of emission pollutants emitted by vehicles. Subsequently, the driving cycles are the tests performed to control these emission pollutants. A brief review on these topics is carried out. Finally, based on the European regulations, a specific vehicle class is selected as the target study.

This chapter is organized as follows. In section 3.1 some important concepts related to the automotive industry are introduced. The vehicles' classification by weight and the driving cycles are analysed in more detail. Section 3.2 presents the vehicle class chosen as target study. This section ends with a simulation performed on each vehicle selected for the target study. These simulations provide the necessary parameters that are required in the next chapter.

3.1 Vehicle classification by weight and driving cycles using the European regulations

This thesis uses the European case study as reference, in line with the European regulations. According to this nomenclature the classification of vehicles by weight is the given in table 3.1. The maximum mass indicated in table 3.1 is also named as the technically permissible maximum mass. This corresponds to the maximum mass with which the vehicle is allowed to drive on road [42]. Another topic of vital

Table 3.1: Vehicle weight classification by the European regulation [41].

Category	Description	Sub-category	Number of persons	Maximum mass (MM)
M	Carriage of Passengers	M1	Up to 9 Persons	
		M2	Over 9 Persons	$\leq$5000 kg
		M3		$>$5000 kg
N	Carriage of Goods	N1	N.A.	$\leq$ 3500 kg
		N2		3500 kg$<$ MM $\leq$12000 kg
		N3		$>$ 12000 kg

importance in the automotive industry are the pollutant emissions. The introduction of a thermoelectric generators in the vehicle's exhaust gas system will influence these emissions. It is expected that the TEG will reduce the fuel consumption and herein decrease the pollutant emission. In order to get a wider notation of the importance and regulation of the emission pollutants a brief review is given next.

The pollutant emissions (HC, CO, NO_x and PM) from road vehicles are regulated separately for light passenger cars and commercial vehicles and for heavy duty vehicles. While the emission standards for light passenger cars and commercial vehicles were introduced in the early 1970s, the first requirements for heavy duty vehicles came in at the end of the 1980's. Over the years, progressively more stringent emission limits have been set at European level to help in bringing down pollution levels.

At present, the emission standards in force for light passenger cars and commercial vehicles are set by Euro 5 and Euro 6, regulation No 715/2007 [43]. This regulation covers vehicles of categories M1, M2, N1 and N2, with a reference mass not exceeding ($\leq$) 2610 kg. The reference mass is defined by [43] as "the mass of the vehicle in running order less the uniform mass of the driver of 75 kg and increased by a uniform mass of 100 kg". In turn the mass of a vehicle in running order is defined by [41] as "the mass of an unladen vehicle with bodywork, and with coupling device in the case of a towing vehicle, or the mass of the chassis with cab if the manufacturer does not fit the bodywork and/or coupling device, including coolant, oils, 90 per cent of fuel, 100 per cent of other liquids except used waters, tools, spare wheel, driver (75 kg) and, for buses and coaches, the mass of the crew member (75 kg) if there is a crew seat in the vehicle." For heavy duty vehicles, Euro VI emission standards were introduced by regulation No 595/2009 [44]. This regulation covers vehicles of categories M1, M2, N1, and N2 with a reference mass exceeding ($>$) 2610 kg and all motor vehicles of categories M3 and N3.

In order to quantify the vehicle emissions presented above, researchers developed a series of methods mostly based on driving cycles. A driving cycle is a representative speed-time profile of a driving behaviour in a specific area. The pollutants emitted by the vehicle when driving these cycles can then be compared to those which could have been expected under the above mentioned directives. This procedure allows for the reliable quantification of the pollutants contained in the exhaust gas from different vehicles in a normalized way.

Driving cycles can be roughly divided into two categories, modal driving cycles and transient driving cycles. The first one is built from combining different phases of idling, constant acceleration/deceleration and steady speed. These cycles are not representative of real driving conditions since they correspond to an unrealistic transition between the different phases in the driving cycle which could result in erroneous emission estimation. Actually a driving cycle should be considered a random process, on the grounds that the relationship of speed-time at any moment in a real driving process is uncertain. Therefore in this master thesis, transient driving cycles are used, since they account for a better representation of the real driving conditions. This cycle represents a speed-time profile based on a real roadway network. Different driving cycles have been developed over the years with each cycle representing a specific type of driving [45]. Nevertheless, this master thesis will only focus on the normalized driving cycles developed and accepted under the vision from the United Nations Economic Commission for Europe (UNECE). For light passenger cars and commercial vehicles the WLTP (Worldwide harmo-

nized Light vehicles Test Procedure) will be used in this master thesis. The WLTP driving cycle is still under development, but will come into force in 2017 [46] and replace the NEDC. The WLTP procedure includes three test cycles applicable to different vehicle categories according to their Power to Mass Ratio (PMR). For the heavy duty vehicles the standardized transient cycle defined by UNECE is the World Harmonized Transient Cycle (WHTC). Contrary to the WLTP, the WHTC is an engine dynamometer test. However since the simulation vehicle program used to obtain the input data for the TEG model takes into account the entire vehicle and not only the engine, the World Harmonized Vehicle Cycle (WHVC) was used. Contrary to the WLTP and WHTC, the WHVC [47] is not a part of the standard international testing procedures, and was developed for research purposes only.

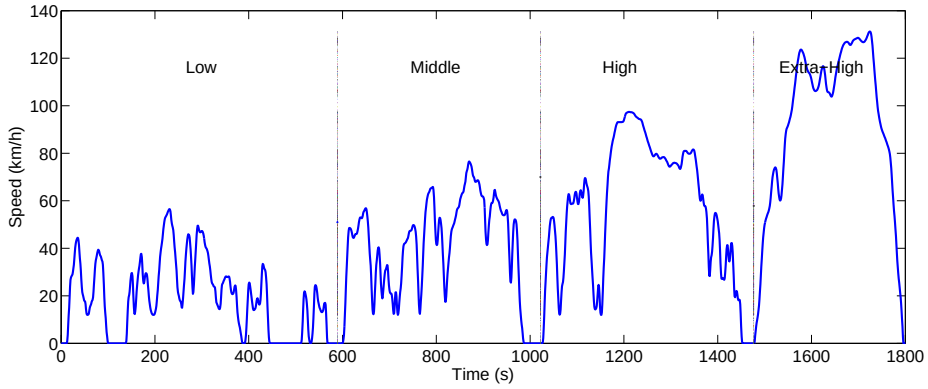

(a) Representation of the european driving cycle WLTC applied to light passenger cars and commercial vehicles in the future.

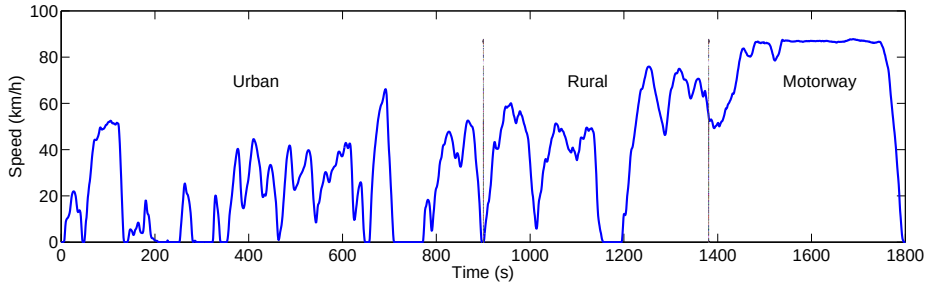

(b) Representation of the chassis dynamometer test WHVC applied to heavy duty vehicles.

Figure 3.1: Representation of two European transient driving cycles.

3.2 Selected target study

Concluding this brief theoretical background related to the automotive sector, the vehicles selected as target study for this master thesis are presented. Table 3.2 summarises the choice of vehicles and the vehicle's respective boundary conditions (i.e. the driving conditions) under which they will be analysed. In table 3.2, vehicle A represents the upper limit of class N1. Vehicle B and C represent the N2 class, where vehicle C represents the upper limit of this class. Vehicles D, E and F represent the N3 class. Vehicle F was chosen as the upper limit of class N3 for conventional guidelines used in the European

Table 3.2: Target Study and respective boundary conditions.

Vehicle	Sub-category	Weight(kg)	Constant speed (km/h)	Driving cycle
A (Vehicle 3.5 tonnes)	N1	3500	120	WLTC
B	N2	9783	90	x
C	N2	12000	90	x
D	N3	14324	90	x
E	N3	26000	90	x
F (Vehicle 40 tonnes)	N	40000	90	WHTC (WHVC)

countries [48].

In order to obtain the required input parameters used in chapter 4 the target study under their boundary conditions presented in table 3.2 where simulated on an advanced vehicle simulator named ADVISOR [49]. This vehicle simulator was developed in MATLAB®/Simulink®[38] and is frequently used by the vehicle engineering community with the primary objective to analyse the overall vehicle system performance.

To carry out the vehicle simulation on ADVISOR, additional information to the one presented in table 3.2 was required namely the vehicles frontal area, the vehicles engine type with specification of the nominal power and maximum torque and the vehicles tire dimensions. Furthermore, the composition of the exhaust gas system needed to be specified to perform the simulation on ADVISOR. The main function of the exhaust gas system is to purify the exhaust gas, of chemical components and particulate matter to fulfil the legal requirements and afterwards discharge them to the atmosphere. The exhaust gas system used to perform the simulation on the vehicles from table 3.2 was composed of a diesel oxidation catalyst (DOC) and a diesel particle filter (DPF). This second component, diesel particle filter, needs to be taken into account since the vehicles presented in table 3.2 are running by a diesel engine.

Subsequently the presented target study in table 3.2 together with the additional vehicles characteristics presented above were simulated by using ADVISOR. The resulting output from these simulations is summarized in table 3.3. Two additional notes about these simulation results need to be made. The temperature presented in table 3.3 represents the temperature measured exactly after the diesel particulate filter. This position represents the location where the TEG is designed to be implemented. Consequently, the exhaust gas temperature shown in table 3.3 represent the one at which the performance of the TEG will be evaluated in the next chapter. The second note that should be pointed out refers to the cooling water temperature. This temperature also was obtained due to the simulations and shows a value of 95ºC for the whole range of simulated vehicles.

Table 3.3: Simulation output results for the target study and their respective boundary conditions presented in table 3.2.

Not available.

A quick analyses of table 3.3 allows to confirm the high mass flow rates from the diesel engines. It is also seen that for a constant speed, the increase of the vehicle weight mass leads to a consequently increases in the mass flow rate as can be seen schematically in figure 3.2.

Not available.

Figure 3.2: Schematic of the influence of the vehicles weight on the exhaust gas mass flow rate.

Until now, gasoline engines used in passenger cars, are preferable for the application of the TEG due their promising high exhaust gas temperature, which clearly enhances the performance of the thermoelectric generator. Although, despite the diesel engines lower exhaust gas temperatures, their considerable higher mass flow rate make these engines also a potential user for TEGs. Additionally, two more facts motivate the application of TEGs on heavy duty vehicles. First, these vehicles when compared to passenger cars do not represent any space problems since they offer a huge space where the TEG could easily be introduced. In addition, the number of driving hours of vehicles for carriage of goods are much higher than that of passenger cars. Subsequently, each percentage of fuel savings for the first mentioned is even more important. In conclusion, these diesel engine vehicles are seen to be a good choice for the application of a TEG.

Chapter 4

Results

Energy is a fundamental concept of thermodynamics and the analysis of energy is one of the most significant engineering analysis. The energy analysis is based on the first law of thermodynamics, which states that energy is conserved and cannot be created or destroyed. In order to reach the goals of a more efficient use of energy resources, an availability analysis, often called exergy analysis, is used. This analysis is based on the second law of thermodynamics and enables the location, the types and true magnitudes of waste and losses to be determined. This is most interesting in engineering when designing thermal systems aiming to reduce the sources of inefficiency. In this chapter both analyses are carried out on the exhaust gas which will enter the TEG. Finally, after knowing the maximum potential which can be extracted from the exhaust gas the TEG performance is analysed.

The chapter is divided as follows. First in section 4.1 an energy and availability analysis is carried out on the exhaust gas from the selected vehicles presented in section 3.2. Afterwards in section 4.2 two vehicles from table 3.2 are selected on which the numerical model developed in chapter 2 is applied. Using this numerical model a parametric study on the heat exchanger is performed. Additionally, the TEG's system and TEG's recovery efficiency is analysed. Finally, in section 4.3 the thermocouple's behaviour in a single state and its influence on the TEG is analysed.

4.1 Potential analyses: Energy and Availability analyses

Not available.

4.2 Parametric study on the heat exchanger

Not available.

4.2.1 Plain fin analysis

Not available.

4.2.2 Geometry variation: Double width and double length analysis

Not available.

4.2.3 Offset strip fin analysis

Not available.

4.2.4 TEG performance

Not available.

4.3 Thermocouple analysis

Not available.

4.3.1 Thermocouple in a single state

Not available.

4.3.2 Interaction between the thermocouple and the TEG

Not available.

Chapter 5

Conclusions

The work presented in this master thesis allows to draw some important conclusions, related to the overall thermoelectric generator performance. However, this thesis is only the foundation for waste heat recovery with a TEG, there is still room for improvement and refinements in the future.

This chapter is organized in two sections. In section 5.1 the main achievements of the research described in the thesis are presented. To finish this chapter, in section 5.2 some directions for future work are pointed out.

5.1 Achievements

Not available.

5.2 Future Work

In this master thesis a numerical model for a thermoelectric generator was developed and a preliminary set of parametric studies were performed on this device. Nevertheless, further refinements on this numerical model are necessary in order to maximize the TEG power while minimizing the system size. Some suggestions are introduced and briefly described as future directions for this work.

- The cold sink of this model could be improved. For this, enhancement structures could be introduced instead of using a simple duct. Their influence on the electrical output power could be evaluated. Also the pumping power for the coolant which in this work has not been considered, should be analysed in future studies.

- The fill factor, F, which is defined as the ratio of the thermoelectric material to the area of the ceramic plate should also be taken into account. For a given available ceramic plate area (set by the heat exchanger dimension), it would be interesting to get the optimum filling fraction, which maximizes the ratio electrical output power to thermoelectric material price.

- Another useful and relevant parameter that could be implemented in the numerical model developed within the course of this master thesis is the weight estimation. The weight estimation is of essential importance in such a preliminary design. To do so, the weight of each TEG component could be computed by using this geometric dimension and their material density. Subsequently, it could be analysed where possible weight reductions are possible and how they influence the overall performance of the TEG.

- The thermoelectric material improvement is itself a huge area of study. A deep material investigation would be out of the principal goal of this branch of study where this master thesis is inserted. Another idea which is suggested and explained next, indirectly takes into account the thermoelectric material's performance. After getting an initial estimate for the temperature decrease along the TEG length, it is suggested to build thermoelectric modules with different materials. These thermoelectric modules made from different materials should then be distributed along the TEG length in order to assure that the material which they are made from is working at its maximum ZT value. Consequently this would improve the performance of each thermoelectric module and increase the overall electrical output power of the TEG.

After getting a first estimation for the additional parameters a deeper analysis should be performed. Some of this "deeper" studies are listed next.

- The thermal and electrical contact resistance which were neglected in this work, need to be analysed carefully, in order to account for the errors that arise from neglecting them. Also, if the obtained errors are significant, the numerical model should be altered in order to account for them.

- The electrical system of the thermoelectric generator needs to be analysed in more detail. In this research area it would be of most benefit to optimize the number of thermocouples per thermoelectric module. Additionally, the thermoelectric module's geometry should be analysed in order to minimize the losses that arise from varying temperatures over the thermoelectric modules, which are caused by the temperature decrease along the TEG length. Another improvement that could be performed, still related to the electrical system of the TEG, is the condition of maximum power. In the numerical model developed the condition, R_L=R_{int} for maximum power was assumed. In reality, however this condition needs to be continuously adjusted. Therefore it would be advantageous to develop a maximum power point tracking, MPPT. The MPPT continuously verifies this condition and subsequently adjusts the load resistance to the thermocouples internal resistance, in order to continuously guaranty the required condition for maximum power, R_L=R_{int}.

- The heat exchangers' geometries which were analysed in this work also need to be improved. After obtaining the first preliminary dimensions of the heat exchanger with this numerical TEG model, it is suggested to study and optimize their behaviour through the use of 3D analyses, e.g. by using the software Fluent. This is of fundamental importance, since the numerical model developed in this work bases on empirical equations, which cannot mirror the real fluid behaviour as accurately as a 3D analysis.

After getting a better understanding of the overall TEG in this “isolated state” a next step would be to analyse how to introduce and use the electrical power from the TEG in the vehicle. Subsequently, after getting this answer, the final step would be to include the numerical TEG model in a numerical model that takes a complete vehicle into account. With this the behaviour of both, the vehicles and the TEGs, could be evaluated together.
In future studies this overall process could be developed and applied in transient conditions.

Bibliography

[1] Bp energy outlook 2035., February 2015.

[2] A. R. D. *A thermoelectric Application to Vehicles*, chapter 56. Taylor and Francis, 2006.

[3] K. Matsubara and M. M. *A thermoelectric Application to Vehicles*, chapter 52. Taylor and Francis, 2006.

[4] J. C. Bass, N. B. Elsner, and F. A. Leavitt. Performance of the 1 kw thermoelectric generator for diesel engines. In *International Conference on Thermoelectrics*, 1994.

[5] K. Ikoma, M. Munekiyo, K. Furuya, M. Kobayashi, T. Izumi, and K. Shinohara. Thermoelectric module and generator for gasoline engine vehicles. In *International Conference on Thermoelectrics*, 1998.

[6] E. F. Thacher, B. T. Helenbrook, M. A. Karri, and C. J. Richter. Testing of an automobile exhaust thermoelectric generator in a light truck. *Journal of Automobile Engineering*, 221:95–107, September 2006.

[7] C. T. Hsu, D. J. Yao, K. J. Ye, and B. Yu. Renewable energy of waste heat recovery system for automobiles. *Journal of Renewable and Sustainable Energy 2*, January 2010.

[8] C. T. Hsu, G. Y. Huang, H. S. Chu, B. Yu, and D. J. Yao. Experiments and simulations on low-temperature waste heat harvesting system by thermoelectric power generators. *Applied Energy*, 88:1291–1297, October 2010.

[9] X. Liu, Y. D. Deng, Z. Li, and C. Q. Su. Performance analysis of wast heat recovery thermoelectric generation system for automotive application. *Energy Conversion and Managment*, 90:121–127, November 2014.

[10] B. D. In and K. H. Lee. A study of a thermoelectric generator applied to a diesel engine. *Journal of Automobile Engineering*, February 2015.

[11] C. Lu, S. Wang, C. Chen, and Y. Li. Effect of heat enhancement for exhaust heat exchanger on the performance of thermoelectric generator. *Applied thermal Engineering*, 89:270–279, 2015.

[12] S. Bai, H. Lu, T. Wu, X. Yin, X. Shi, and L. Chen. Numerical and experimental analysis for exhaust heat exchangers in automobile thermoelectric generators. *Case Studies in Thermal Engineering*, 4:99–112, July 2014.

[13] H. Lu, T. Wu, S. Bai, K. Xu, Y. Huang, W. Gao, X. Yin, and L. Chen. Experiment on thermal uniformity and pressure drop of exhaust heat exchanger for automotive thermoelectric generator. *Energy*, 54:372–377, April 2013.

[14] X. Liu, Y. D. Deng, K. Zhang, M. Xu, Y. Xu, and C. Q. Su. Experiments and simulations on the heat exchangers in thermoelectric generator for automotive application. *Applied Thermal Engineering*, 71:364–370, 2014.

[15] C. Q. Su, W. S. Wang, X. Liu, and Y. D. Deng. Simulation and experimental study on thermal optimization of the heat exchanger for automotive exhaust-based thermoelectric generators. *Case Studies in Thermal Engineering*, 4:85–91, June 2014.

[16] M. Zhou, Y. He, and Y. Chen. A heat transfer numerical model for thermoelectric generator with cyclindrical shell and straight fins under steady-state conditions. *Applied Thermal Engineering*, 68: 80–91, 2014.

[17] Z. Niu, S. Yu, H. Diao, Q. Li, K. Jiao, Q. Du, H. Tian, and G. Shu. Elucidating modeling aspects of thermoelectric generator. *International Journal of Heat and Mass Transfer*, 85:12–32, January 2015.

[18] A. Adelkefi, A. Alothman, and M. R. Hajj. Performance analysis and validation of thermoelectric energy harvesters. *Smart Materials and Structures*, 22(9), August 2013.

[19] M. Chen, L. A. Rosendahl, T. J. Condra, and J. K. Pedersen. Numerical modeling of thermoelectric generatos with varing material properties in a circuit simulator. *Transactions on Energy Conversions*, 24:112–124, March 2009.

[20] S. Yu, Q. Du, H. Diao, G. Shu, and K. Jiao. Effect of vehicle driving conditions on the performance of thermoelectric generator. *Energy Conversion and Managment*, 96:363–376, March 2015.

[21] Hi-z. Hz-20 thermoelectric module., 2015-10-8. URL `http://www.hi-z.com/hz-20.html`.

[22] X. Gou, S. Yang, H. Xiao, and Q. Qu. A dynamic model for thermoelectric generator applied in waste heat recovery. *Energy*, 52:201–209, February 2013.

[23] D. Tatarinov, M. Koppers, G. Bastian, and D. Schramm. Modeling of a thermoelectric generator for thermal energy regeneration in automobiles. *Journal of Electronics Materials*, 22, June 2013.

[24] S. Kumar, S. D. Heister, X. Xu, J. R. Salvador, and G. P. Meisner. Thermoelectric generators for automotive waste heat recovery systems part i: Numerical modeling and baseline model analysis. *Journal of Electronics Materials*, 42:665–674, February 2013.

[25] S. Kumar, S. D. Heister, X. Xu, J. R. Salvador, and G. P. Meisner. Thermoelectric generators for automotive waste heat recovery systems part ii: Parametric evaluation and topological studies. *Journal of Electronics Materials*, 42:944–955, March 2013.

[26] Y. Wang, C. Dai, and S. Wang. Theoretical analysis of a thermoelectric generator using exhaust gas of vehicles as heat source. *Applied Energy*, 112:1171–1180, February 2013.

[27] H. Lee. *Thermal Design: Heat Sinks, Thermoelectrics, Heat Pipes, Compact Heat Exchangers, and Solar Cells.* John Wiley and Sons, 2010.

[28] F. P. Incorpera, D. P. Dewitt, T. L. Bergman, and A. S. Lavine. *Introduction to Heat Transfer.* John Willey and Sons, 2007.

[29] E. A. Foumeny and P. J. Heggs. *Heat exchange Engineering*, volume Volume 2: compact heat exchangers:techniques of size reduction. Ellis Horwood, 1991.

[30] V. Gnielinski. *Heat transferin Pipe Flow*, chapter G1. Springer, 2010.

[31] W. M. Kays and A. L. London. *Compact Heat Exchangers*. National Press, 1955.

[32] R. M. Manglik and A. E. Bergles. Heat transfer and pressure drop correlations for the retangular offset strip fin compact heat exchanger. *Experimental Thermal and Fluid Science*, 10:171–180, 1995.

[33] M. Kim, J. Lee, S. J. Yook, and K. S. Lee. Correlations and optimization of a heat exchnager with offset-strip fins. *International Journal of Heat and Mass transfer*, 3:1306–1312, January 2011.

[34] Y. Yang and L. Y. General prediction of the thermal hydraulic performance for plate-fin heat exchnager with offset strip fins. *International Journal of Heat and Mass transfer*, 78:860–870, August 2014.

[35] F. M. Walters. Hypersonic research engine project-phase iia, category i. *Test Report on Fin Heat Transfer and Pressure Drop Testing*, 1969.

[36] A. L. London and R. K. Shah. Offset retangular plate-fin surfaces. *Heat Transfer and Flow friction Characteristics*, 90:218–228, 1968.

[37] C. Junior. Analyses thermoelektrischer module und gesamtsysteme. *Technische Universität Carolo-Willhelmina zu Brauschweig*, 2010.

[38] MatthWorks. Matlab. URL `http://www.mathworks.com/`.

[39] X. X. Li, J. Q. Li, F. S. Liu, W. Q. Ao, H. T. Li, and L. C. Pan. Enhanced thermoelectric properties of $(bi_{0.001}pb_{0.999}te)_{0.88}(pbs)_{0.12}$ composites by bi doping. *Journal of Alloys and Compounds*, 547: 86–90, September 2012.

[40] B. Du, H. Li, J. Xu, X. Tang, and C. Uher. Enhanced thermoelectric performance and novel nanopores in $agsbte_2$ prepared by met spinning. *Jornal of Solid State Chemistry*, 184:109–114, November 2010.

[41] UNECE. Classification and definition of vehicles, 2015-10-8. URL `http://www.unece.org/trans/main/wp29/wp29wgs/wp29gen/wp29classification.html`.

[42] EUR-Lex. Commission directive 2003/19/ec of 21 march 2003, 2015-10-8. URL http://eur-lex.europa.eu/legal-content/EN/TXT/HTML/?uri=CELEX:32003L0019&from=EN1.

[43] EUR-Lex. Regulation (ec) no 715/2007, 2015-10-8. URL http://eur-lex.europa.eu/legal-content/EN/TXT/?qid=1440923377867&uri=CELEX:32007R0715.

[44] EUR-Lex. Regulation (ec) no 595/2009, 2015-10-8. URL http://eur-lex.europa.eu/legal-content/EN/TXT/?qid=1440307043541&uri=CELEX:32009R0595.

[45] T. J. Barlow, S. Latham, I. S. McCrae, and P. G. Boulter. *A refrence book of driving cycles for use in the measurement of road vehicle emissions.* TRL, 2009.

[46] E. Economic and S. Committee. Opinion of the european economic and social committee on the 'proposal for a regulation of the european parliament and of the council amending regulations (ec) no 715/2007 and (ec) no 595/2009 as regards the reduction of pollutant emissions from road vehicles', 2015-10-08. URL http://eur-lex.europa.eu/legal-content/EN/TXT/HTML/?uri=CELEX:52014AE1604&rid=2l.

[47] DieselNet. World harmonized vehicle cycle, 2015-10-8. URL https://www.dieselnet.com/standards/cycles/whvc.php.

[48] I. T. Forum. Permissible maximum weights of lorries in europe, 2015-10-8. URL http://www.internationaltransportforum.org/IntOrg/road/dimensions.html/#.

[49] K. B. Wipke, M. R. Cuddy, and S. D. Burch. Advisor 2.1: A user-freindly advanced powertrain simuation using combined backward/forward approach. *National Renewable Energy Laboratory*, 1999.

[50] M. J. Moran and H. N. Shapiro. *Fundamentals of Engineering Thermodynamics.* John Wiley and Sons, 1998.

[51] K. W. Li. *Applied Thermodynamics, Availability Method and Energy Conversion*. Taylor and Francis, 1996.

[52] A. E. T. Group. Austenitic stainless steel (316), 2015-10-8. URL http://www-ferp.ucsd.edu/LIB/PROPS/PANOS/ss.html.

[53] A. E. T. Group. Aluminium oxide, 2015-10-8. URL http://www-ferp.ucsd.edu/LIB/PROPS/PANOS/al2o3.html.

[54] A. E. T. Group. Pure copper, 2015-10-8. URL http://www-ferp.ucsd.edu/LIB/PROPS/PANOS/cu.html.

[55] X. Zhang and L. D. Zhau. Thermoelectric materials: Energy conversion between heat and electricity. *Journal of Materiomics*, 1:92–105, April 2015.

[56] F. Li, X. Huang, Z. Sun, J. Ding, J. Jiang, W. Jiang, and L. Chen. Enhanced thermoelectric properties of n-type bi_2te_3-based nanocomposite fabricated by spark plasma sintering. *Journal of Alloys and Compounds*, 509:4769–4773, February 2011.

[57] X. Guo, X. Jia, J. Qin, H. Sun, Y. Zhang, B. Sun, B. Liu, and H. Ma. Fast preparation and high thermoelectric performance of the stable $bi_{0.5}sb_{1.5}te_3$ bulk materials for differnt synthesis pressures. *Chemical Physics Letters*, 610-611:204–208, July 2014.

[58] Thermal-Fluids-Central. Thermophysical properties: Air at 1atm, 2015-10-8. URL `http://www.thermalfluidscentral.org/encyclopedia/index.php/Thermophysical_Properties:_Air_at_1_atm`.

[59] Z. Niu, H. Diao, S. Yu, K. Jiao, Q. Du, and G. Shu. Investigation and design optimization of exhaust-based thermoelectric generator system for internal combustion engine. *Energy Conversion and Management*, 85:85–101, June 2014.

[60] Z. Niu, Q. Li, W. He, Y. Huo, and K. Jiao. Design optimization of automobile exhaust thermoelectric generator for waste heat recovery. *International Heat Transfer Conference*, 2014.

[61] DCL. Oxidation catalytic purifier dimensions, 2015-10-8. URL `http://www.dcl-inc.com/about-us/`.

[62] D. M. Rowe and G. Min. Design theory of thermoelectric modules for electrical power generation. *Science, Measurment and Technology*, 143:351–356, November 1996.